

Similar or Totally Different: The Control of Conjugation Degree through Minor Structural Modifications, and Deep-Blue Aggregation-Induced Emission Luminogens for Non-Doped OLEDs

Jing Huang, Ning Sun, Yongqiang Dong, Runli Tang, Ping Lu, Ping Cai, Qianqian Li, Dongge Ma,* Jingui Qin, and Zhen Li*

Four 4,4'-bis(1,2,2-triphenylvinyl)biphenyl (BTPE) derivatives, 4,4'-bis(1,2,2-triphenylvinyl)biphenyl, 2,3'-bis(1,2,2-triphenylvinyl)biphenyl, 2,4'-bis(1,2,2-triphenylvinyl)biphenyl, 3,3'-bis(1,2,2-triphenylvinyl)biphenyl and 3,4'-bis(1,2,2-triphenylvinyl)biphenyl (*o*TPE-*m*TPE, *o*TPE-*p*TPE, *m*TPE-*m*TPE, and *m*TPE-*p*TPE, respectively), are successfully synthesized and their thermal, optical, and electronic properties fully investigated. By merging two simple tetraphenylethene (TPE) units together through different linking positions, the π -conjugation length is effectively controlled to ensure the deep-blue emission. Because of the minor but intelligent structural modification, all the four fluorophores exhibit deep-blue emissions from 435 to 459 nm with Commission Internationale de l'Eclairage (CIE) chromaticity coordinates of, respectively, (0.16, 0.14), (0.15, 0.11), (0.16, 0.14), and (0.16, 0.16), when fabricated as emitters in organic light-emitting diodes (OLEDs). This is completely different from BTPE with sky-blue emission (0.20, 0.36). Thus, these results may provide a novel and versatile approach for the design of deep-blue aggregation-induced emission (AIE) luminogens.

1. Introduction

Considerable interest has been attracted to the research field of organic light-emitting diodes (OLEDs) due to their vast

J. Huang, R. Tang, Dr. P. Cai, Dr. Q. Li,
Prof. J. Qin, Prof. Z. Li
Department of Chemistry
Wuhan University
Wuhan 430072, China
E-mail: lizhen@whu.edu.cn; lichemlab@163.com

N. Sun, Prof. D. Ma
Institute of Applied Chemistry
The Chinese Academy of Sciences
Changchun 130022, China
E-mail: mdg1014@ciac.jl.cn

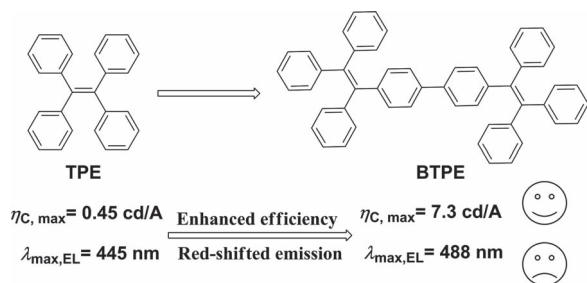
Prof. Y. Dong
Department of Chemistry
Beijing Normal University
Beijing 100875, China

Dr. P. Lu
Department of Chemistry
Jilin University, Jilin 130022, China

DOI: 10.1002/adfm.201202639



applications in display and lighting.^[1] Despite the great success achieved by some commercial products in this area, a critical drawback to realizing full-color displays is the poor performance of deep-blue OLEDs, since the intrinsic wide bandgap makes it very difficult to inject charges into the blue emitters.^[2,3] During the past decade, a number of excellent fluorescent blue light-emitting materials, composed of anthracene,^[4] fluorene,^[5] and styrylarylene^[6] derivatives, have been reported in the literature. Shu et al.^[7] and Cheng et al.^[2a] developed efficient non-doped deep-blue OLEDs with luminescence efficiencies of up to 5.3 and 5.6 cd A⁻¹. Generally, when fabricated as thin solid films in practical applications, most fluorophores suffer from the notorious aggregation-caused quenching (ACQ) effect.^[8] In 2001, Tang's group discovered an "abnormal" phenomenon, termed aggregation-induced emission (AIE), which has been proved to be an effective approach to tackle the ACQ problem:^[9] a series of organic molecules were found to be non-luminescent in the solution state but highly emissive in the aggregated state.^[10] Among the typical AIE luminogens, tetraphenylethene (TPE) and many of its derivatives (Chart S1 in the Supporting Information) enjoy the advantages of facile synthesis and outstanding AIE effect.^[11] However, it is a pity that none of them is an efficient emitter in the deep-blue region, although TPE itself is a weak one. The most promising example, 4,4'-bis(1,2,2-triphenylvinyl)biphenyl (BTPE) (Scheme 1), constructed by two simple TPE units, exhibited outstanding improvement in its electroluminescence (EL) performance, with current efficiency of up to 7.3 cd A⁻¹ (0.45 cd A⁻¹ for TPE), well demonstrating the proverb "two is better than one";^[12] however, unfortunately, the maximum EL emission wavelength is red-shifted to a large extent, from 445 (deep-blue) to 488 nm (sky-blue). Is it possible to retain the deep-blue emission of TPE, while improving its low efficiency of 0.45 cd A⁻¹ dramatically, just by modifying the subtle structure of the luminophors? If it is the case, many better AIE emitters could be developed, and the properties of the present

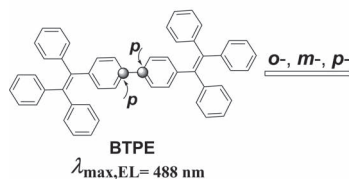


Scheme 1. Chemical structures and EL performances of TPE and BTPE.

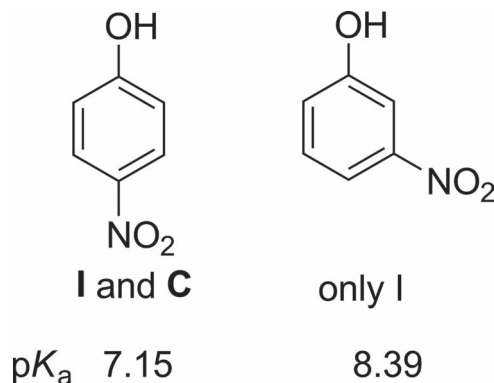
huge number of TPE-based luminophors should be re-evaluated upon minor structural adjustments.

Very recently, we reported several TPE-based blue emitters achieving a balance between emission efficiency and prolonged π -conjugation^[13] (Chart S2 in the Supporting Information). Our synthetic ideas are the linkage of TPE to the classical and efficient blue moiety spirofluorene by sharing one phenyl ring or linking with carbazole through the single carbon–nitrogen bond to ensure good EL performance and blue emission, or the utilization of the twisted conformation to effectively decrease the conjugation degree. Both of the methods have partially realized our idea of generating blue AIE luminogens, however, efficient emitters with deep-blue emission remain a challenge.^[14] Analyzing the previous cases carefully, on one side the introduction of the additional aromatic rotators could improve the LED efficiency of TPE moieties; meanwhile, on another side, the bonded aromatic moieties would extend the formed π -conjugation system, leading to the bathochromic shift of the emission. Our examples could decrease the π -conjugation between TPE and the introduced aromatic rings to a large degree; thus, the luminophors could emit blue light, similar to TPE itself. If the π -conjugation degree between the aromatic blocks in the newly designed TPE-based luminophors could be further decreased, for example, to the extent that it would almost be negligible, perhaps emission in the deep-blue region could be achieved. Towards this goal, further structural modification should be considered carefully, in addition to our previous two methods mentioned above.

Any textbook of basic organic chemistry will indicate that different positions of nitro and hydroxyl groups in nitrophenols, as **Scheme 2** illustrates, will surely affect their pK_a values. Interestingly, in *m*-nitrophenol, the conjugated effect could be nearly ignored between the two groups, while in *p*-nitrophenol, it cannot. Inspired by this point, it is expected that just by changing the linkage mode of two TPE moieties in BTPE, the effect of “two is better than one” should be still present; more importantly, the emission might possibly remain almost the same as for TPE itself, as the result of the much decreased conjugated effect between the two TPE moieties, with the linkage mode of *meta*-position possibly being the favorite.



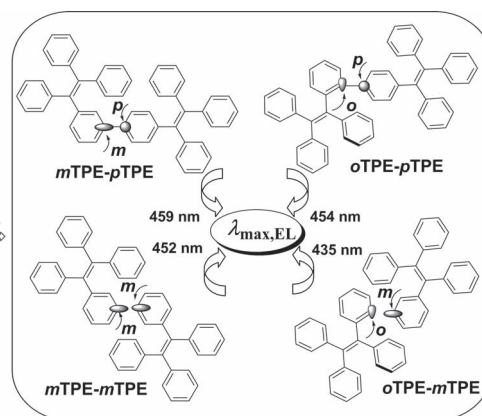
Scheme 3. Chemical structures of *mTPE-pTPE*, *mTPE-mTPE*, *oTPE-mTPE*, and *oTPE-pTPE*.

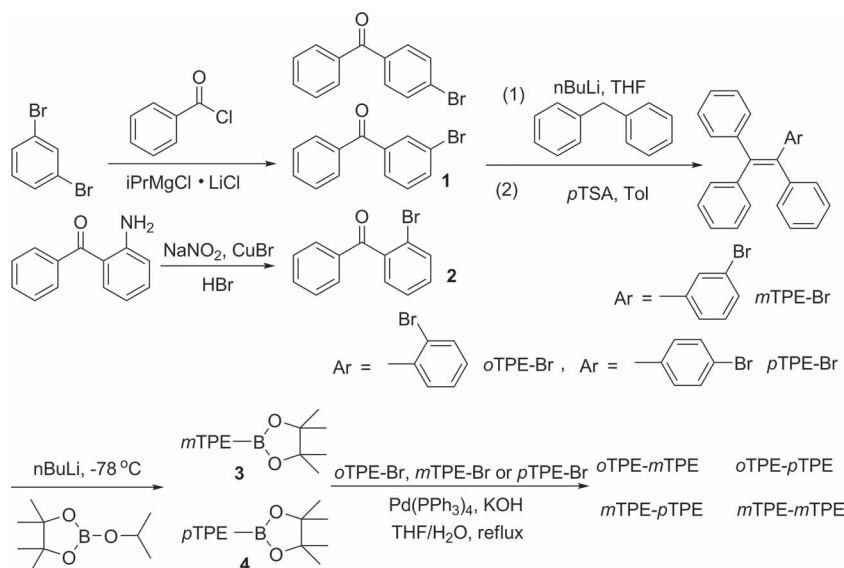


I = Inductive effect
C = Conjugated effect

Scheme 2. The inductive and/or conjugative effect exists in *m*- and *p*-nitrophenol.

Accordingly, four BTPE derivatives, *oTPE-mTPE*, *oTPE-pTPE*, *mTPE-mTPE*, and *mTPE-pTPE* (**Scheme 3**) were synthesized by utilizing the different conjugated effects of *ortho*-, *meta*-, and *para*- linkages of biphenyl. In other words, when two TPE units are merged with different linking positions, the prolonged π -conjugation length could be partially shortened for bluer emission, compared to BTPE with sky-blue emission. The experimental results largely confirmed our ideas: when fabricated as emitters in OLEDs without optimization, all the four fluorophores exhibit deep-blue emissions from 435 to 459 nm with Commission Internationale de l'Éclairage (CIE) chromaticity coordinates of (0.16, 0.14), (0.15, 0.11), (0.16, 0.14), and (0.16, 0.16), totally different from BTPE with sky-blue emission (0.20, 0.36). The highest L_{max} is up to 2.8 cd A^{-1} , much higher than that of TPE (0.45 cd A^{-1}). Though the device performance is inferior to those of the best deep-blue emitters, we believe that excellent EL efficiencies could be obtained through further device optimization and structure modification. Herein, we present the synthesis, photophysical properties, and electroluminescence of the four BTPE derivatives in detail.





Scheme 4. Synthetic routes to BTPE derivatives *mTPE-pTPE*, *mTPE-mTPE*, *oTPE-mTPE*, and *oTPE-pTPE*.

2. Results and Discussion

2.1. Synthesis

Scheme 4 illustrates the synthetic routes to the four BTPE derivatives of *oTPE-mTPE*, *oTPE-pTPE*, *mTPE-mTPE*, and *mTPE-pTPE*. Unlike commercially available 4-bromobenzophenone, its two isomers, 3-bromobenzophenone (**1**) and 2-bromobenzophenone (**2**), were synthesized through two different approaches. While compound **1** was obtained from the reaction between 1,3-dibromobenzene and benzoyl chloride, the 2-aminobenzophenone was converted to compound **2** in two steps, with the diazo moieties as the reactive intermediate. Subsequently, the obtained compounds of **1** and **2**, and the purchased 4-bromobenzophenone, reacted with diphenylmethane, to yield the corresponding bromo-TPEs, including *pTPE-Br*, *mTPE-Br*, and *oTPE-Br*. Next, these three bromo-TPEs were utilized to synthesize their corresponding TPE boronic esters. While the TPE boronic esters **3** and **4** were prepared smoothly, the boronic ester with the substituted position in the ortho-position could not be obtained, although we tried several times with various efforts to optimize the reaction conditions; the main reason might be the relatively too-large steric effect. Next, the Suzuki coupling reactions, catalyzed by $\text{Pd}(\text{PPh}_3)_4$, of TPE boronic esters with *pTPE-Br*, *mTPE-Br*, and *oTPE-Br*, gave the final products of four BTPE derivatives: *oTPE-mTPE*, *oTPE-pTPE*, *mTPE-mTPE*, and *mTPE-pTPE*. Without the corresponding boronic ester, the compound *oTPE-oTPE* could not be prepared; however, the study of its isomers could well demonstrate their almost totally different properties. The obtained four BTPE derivatives, just like BTPE, contain two pieces of TPE blocks, differing in their linkage modes, which directly leads to their having different properties, as mentioned above and discussed in detail in the following. It should be pointed out that the whole synthetic route was not too hard, and the designed

TPE boronic esters (**3** and **4**) were key reactive intermediate. It is not difficult to think that some other AIE compounds containing TPE blocks could be easily prepared from the TPE boronic esters **3** and **4** with other aromatic halides; in such AIE compounds, the conjugated effects between the TPE blocks and the chosen aromatic rings, could perhaps be controlled, to a large degree, to adjust their light-emitting properties, especially the emission color. From this point, the syntheses presented here might stimulate the preparation of more interesting AIE molecules; as a good illustration, many other TPE derivatives with different linkage modes are being tested in our laboratory.

The four BTPE derivatives, *oTPE-mTPE*, *oTPE-pTPE*, *mTPE-mTPE*, and *mTPE-pTPE*, were fully characterized by ^1H and ^{13}C NMR spectroscopy, mass spectrometry, and elemental analysis, well confirming their molecular structures. Fortunately, single crystals of *oTPE-mTPE* and *oTPE-pTPE* were cultured

from their dichloromethane/methanol solutions and crystallographically characterized.

2.2. Thermal Properties

To be a good emitter, the luminogen should possess good thermal properties to ensure the process of vacuum deposition and subsequent operating stability of the devices. The thermal properties of the four BTPE derivatives were investigated by thermal gravimetric analyses (TGA; **Figure 1**) and differential

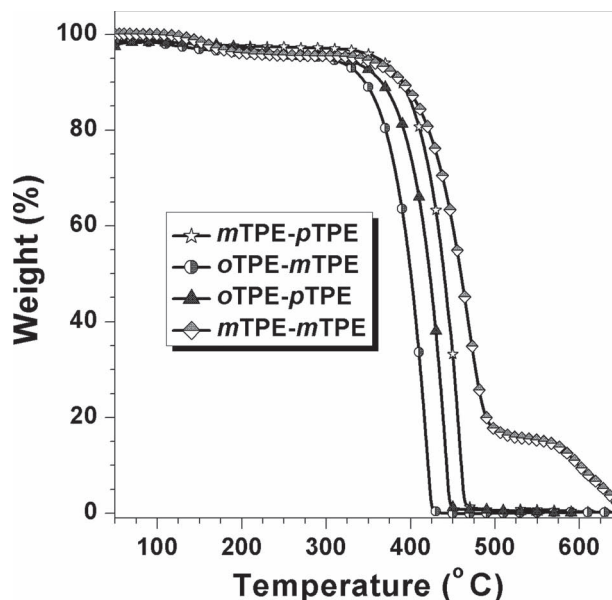


Figure 1. TGA thermograms of *mTPE-mTPE*, *mTPE-pTPE*, *oTPE-mTPE*, and *oTPE-pTPE* recorded under N_2 at a heating rate of 10 °C min^{-1} .

Table 1. The thermal, electrochemical and photophysical data of *m*TPE-*p*TPE, *m*TPE-*m*TPE, *o*TPE-*m*TPE, and *o*TPE-*p*TPE.

	$T_d^{a)}$ [°C]	T_g [°C]	$E_g^{b)}$ [eV]	$E_{HOMO}^{c)}$ [eV]	$E_{LUMO}^{d)}$ [eV]	$\lambda_{max,ab}^{e)}$ [nm]	PL $\lambda_{max}^{(aggr)}^{f)}$ [nm]
<i>o</i> TPE- <i>p</i> TPE	310	–	3.27	5.47	2.20	318	473
<i>o</i> TPE- <i>m</i> TPE	302	99	3.30	5.50	2.20	312	469
<i>m</i> TPE- <i>p</i> TPE	360	114	3.27	5.48	2.21	318	473
<i>m</i> TPE- <i>m</i> TPE	330	–	3.32	5.50	2.18	311	465

^{a)}5% weight loss temperature measured by TGA under N₂; ^{b)}bandgap estimated from optical absorption band edge of the solution; ^{c)}calculated from the onset oxidation potentials of the compounds; ^{d)}estimated using the empirical equation $E_{LUMO} = E_{HOMO} + E_g$; ^{e)}observed from absorption spectra in dilute THF solution; ^{f)}determined in THF/H₂O = 1:99 solution.

scanning calorimetry (DSC). As listed in **Table 1**, the thermal decomposition temperatures (T_d , corresponding to 5% weight loss) were determined to range from 302 to 360 °C. Due to the bulky TPE unit and more planar structure, *m*TPE-*p*TPE possessed the highest thermal stability and exhibited higher glass transition temperature (T_g) of 114 °C, compared to the other three molecules with more twisted conformation. The good thermal stability, with high T_d and T_g values, should contribute to the preparation of homogeneous and stable amorphous emissive layers in OLED devices.

2.3. Optical Properties

All four BTPE derivatives are soluble in common solvents, such as tetrahydrofuran (THF), chloroform, and dichloromethane, but insoluble in water. **Figure 2A** shows the absorption spectra of *m*TPE-*p*TPE, *m*TPE-*m*TPE, *o*TPE-*p*TPE, and *o*TPE-*m*TPE in dilute THF solution, with the maximum absorption wavelengths ($\lambda_{max,abs}$) at 318, 311, 318, and 312 nm, respectively. In comparison with that of BTPE (340 nm), the much blue-shifted $\lambda_{max,abs}$, as much as 29 nm, indicates the shorter conjugation in these four luminogens, which is consistent with our idea of

controlling the conjugated length in the AIE molecules through the effective structural modification of different linkage positions. That is to say, really, we could adjust the electronic structure of the BTPE derivatives to a large extent simply by changing the linkage positions of the two pieces of TPE blocks.

In order to investigate the AIE properties of the new compounds, PL spectra were recorded; THF and water were chosen as the solvent pair for their miscibility. **Figure S1** (Supporting Information) clearly demonstrates the PL change and fluorescent image of *m*TPE-*m*TPE in THF and THF/water mixtures as an example. It is easily seen that, in dilute THF solution, the PL curve is practically a flat line parallel to the abscissa, confirming the nearly non-emissive property in the solution state. However, when a large amount of water is added, intense emission is observed. As shown in **Figure S1** (Supporting Information), when the water fraction is over 80%, the PL intensity increases swiftly, indicating the formation of aggregates. At a f_w value of 99%, the PL intensity is 274-fold higher than that in pure THF. Interestingly, the PL spectrum peak is blue-shifted from 480 to 465 nm as the water fraction increases from 80% to 99%. This could be explained by the morphological change of the aggregates from amorphous to crystalline state; that is, crystallization causes blue-shifted emission, similar to those reported

in the literature.^[11a,15] In our previous work, the more twisted the conformation the AIE molecule, the easier it is to crystallize. For example, Ph3TPE is more easily crystallized than the other two compounds, Ph2TPE and PhTPE, owing to its twisted conformation (**Chart S2** in the Supporting Information). Furthermore, in its LED device, Ph3TPE exhibits much blue-shifted (ca. 27 nm) maximum emission than that in the solutions with the mixture solvents of THF and water. Here, in comparison with BTPE, these four derivatives are more twisted, thus, they are liable to crystallize in the solid states. The blue-shifted emission from 480 to 465 nm, is just a hint for their further blue-shifted emission in LED devices. The EL spectrum will be discussed later. The quantitative enhancement of emission was evaluated by the PL quantum yields (Φ_f), using 9,10-diphenylanthracene as the standard. From pure solution in THF to aggregate state in 99% aqueous

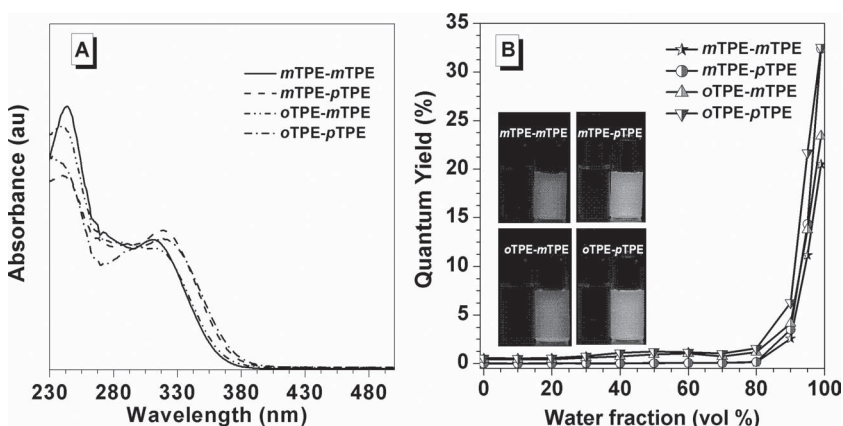


Figure 2. A) UV spectra in THF solution. Concentration (μ M): 12.7, 10.3, 11.6, and 11.2 for *m*TPE-*m*TPE, *m*TPE-*p*TPE, *o*TPE-*m*TPE, and *o*TPE-*p*TPE, respectively. B) Plots of fluorescence quantum yields determined in THF/H₂O solutions using 9,10-diphenylanthracene ($\Phi = 90\%$ in cyclohexane) as standard versus water fractions; inset: photos of *m*TPE-*m*TPE, *m*TPE-*p*TPE, *o*TPE-*p*TPE, and *o*TPE-*m*TPE in THF/water mixtures ($f_w = 0\%$ and 99%) taken under the illumination of a 365 nm UV lamp.

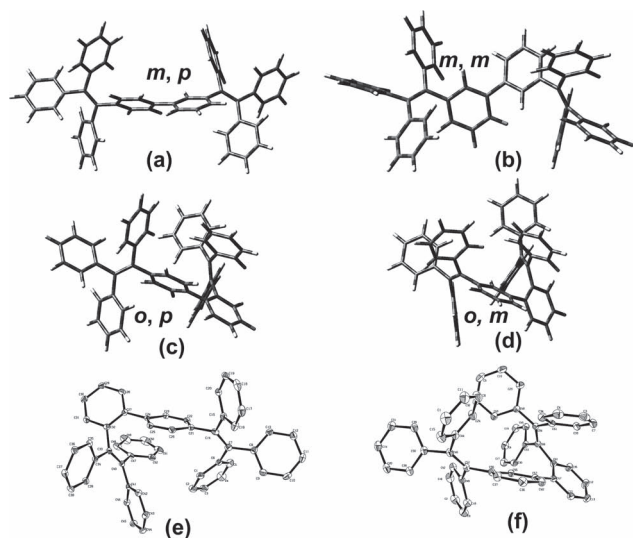


Figure 3. Optimized molecular structures of: a) *mTPE-pTPE*, b) *mTPE-mTPE*, c) *oTPE-pTPE*, and d) *oTPE-mTPE*. ORTEP drawings and bond lengths of: e) *oTPE-pTPE*, and, f) *oTPE-mTPE*.

mixture, the Φ_F values of *mTPE-mTPE* increased from 0.02% to 20.5%. Similar behavior was observed for the other three molecules (Figure 2B and Figure S2–S4 in the Supporting Information). The quantum yields are up to 32.4%, 32.6%, and 23.4%, respectively, for *mTPE-pTPE*, *oTPE-pTPE*, and *oTPE-mTPE* in 99% aqueous mixture, from being nearly nonluminescent in the solution state. In other words, all the compounds are AIE-active.

2.4. Theoretical Calculations and Crystal Structures

To better understand the correlation between structure and physical properties, as well as the device performance, density functional theory (DFT) calculations (B3LYP/6-31g*) were carried out to obtain orbital distributions of highest occupied molecular orbital (HOMO) and lowest unoccupied molecular orbital (LUMO) energy levels and optimized molecular structures. As shown in Figure 3, the optimized molecular structures of these four BTPE derivatives are highly twisted. As mentioned above, the highly twisted conformations make them change easily from the amorphous to the crystalline state. This is another reason for the much blue-shifted emission of the four BTPE derivatives in their LED devices, in comparison with BTPE, in addition to the controlled conjugated effect. Fortunately, we could further examine the geometric structures of *oTPE-pTPE* and *oTPE-mTPE* in their ORTEP drawings, since we obtained their single crystals. As shown in Figure 3, both of these two molecules adopt twisted conformations and no intermolecular interactions exist in the packing arrangement, which is beneficial to prevent the formation of species detrimental to emission. It seems that their twisted extents are larger than those of TPE and BPTPE (Figure S5 in the Supporting Information). Comparing the ORTEP drawings of *oTPE-pTPE* and *oTPE-mTPE* with their calculated optimized structures (Figure 3), they seem

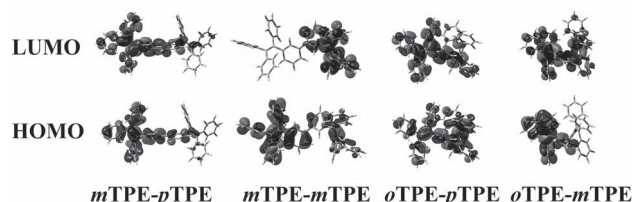


Figure 4. Calculated molecular orbital amplitude plots of HOMO and LUMO levels of *mTPE-pTPE*, *mTPE-mTPE*, *oTPE-pTPE*, and *oTPE-mTPE*.

similar, indicating that the calculated structures could somehow be used to know some molecular information.

According to the single crystal data of *oTPE-pTPE* and *oTPE-mTPE*, the $C_{sp^2}=C_{sp^2}$ double bonds of *oTPE-pTPE* are 1.342 and 1.355 Å, apparently shorter than those in *oTPE-mTPE*, which are 1.351 and 1.360 Å. Analyzing the bond lengths of *oTPE-pTPE* and *oTPE-mTPE* carefully, as shown in Figure S6 (Supporting Information), in comparison with the bond lengths of TPE, the length changes in *oTPE-mTPE* are smaller than those of *oTPE-pTPE*. This discloses that the *oTPE-pTPE* is more conjugated than *oTPE-mTPE*, owing to the different conjugated effect of *para*- and *meta*-linkage modes. This is reasonable: with lesser or negligible electronic conjugated effect between the two TPE blocks in *oTPE-mTPE* and *oTPE-pTPE*, each TPE block should possess similar structure to the TPE molecule itself; thus, the TPE blocks in the BTPE derivatives should have similar bond lengths as in the TPE molecule. It is easily seen that in *oTPE-mTPE*, the bond lengths are more approximate to those of TPE, indicating that the two TPE blocks retain almost the same electronic properties as TPE, no matter that they are linked together through a single carbon–carbon bond. Thus, its emission should be close to that of TPE. Actually, the maximum emission wavelength in its LED device (435 nm) is in the deep-blue region, blue-shifted even compared to TPE, as a result of the more twisted conformation.

Although we have not obtained single crystals of *mTPE-pTPE* and *mTPE-mTPE*, we may estimate that the conjugation length of *mTPE-pTPE* is longer than *mTPE-mTPE*, for the same reason just discussed. These results are well consistent with the measured optical data and realize our idea of tuning the conjugation length for bluer emission by simply changing the linking positions.

Moreover, we carried out theoretical calculations of the four luminogens in order to further understand the structure–property relationship at the molecular level. Figure 4 shows the orbital distributions of HOMO and LUMO energy levels of the four BTPE derivatives. The electron clouds of the HOMOs and LUMOs are almost dominated by the whole molecules, showing the weak intramolecular charge transfer of these luminophores. Thus, the nonpolar properties of these AIE molecules partially ensure their deep-blue emissions in their LED devices.

2.5. Electrochemical Properties

The electrochemical properties of the four BTPE derivatives were investigated by cyclic voltammetry (CV). The HOMO

energy levels were calculated to be about 5.5 eV, according to the following equation: $\text{HOMO} = -(4.8 + E_{\text{ox}})$ eV. Their LUMOs could be obtained from optical bandgap energies (estimated from the onset wavelength of their UV absorptions) and HOMO values, which were about 2.2 eV. The slight difference of their energy levels suggests that these four luminogens possess almost the same transporting properties.

2.6. Electroluminescence

The good thermal property and outstanding AIE effect of the four BTPE derivatives prompted us to investigate their electroluminescence properties. Non-doped OLED devices with a configuration of ITO/MoO₃ (10 nm)/NPB (60 nm)/emission layer (EML) (15 nm)/TPBi (35 nm)/LiF (1 nm)/Al (100 nm) were fabricated. In these OLED devices, MoO₃, NPB, and TPBi worked as the hole-injection, hole-transporting, and hole-blocking layers, respectively, and *o*TPE-*m*TPE, *o*TPE-*p*TPE, *m*TPE-*m*TPE, or *m*TPE-*p*TPE served as emitters.

Figure 5 shows the current density–voltage–brightness (*J*–*V*–*L*) characteristics, current efficiency versus current density curves, and EL spectra of the OLEDs. As listed in Table 2, all the devices turn on at a low voltage from 3.7 to 4.1 V, showing small injection barriers from transporting layers in the devices.

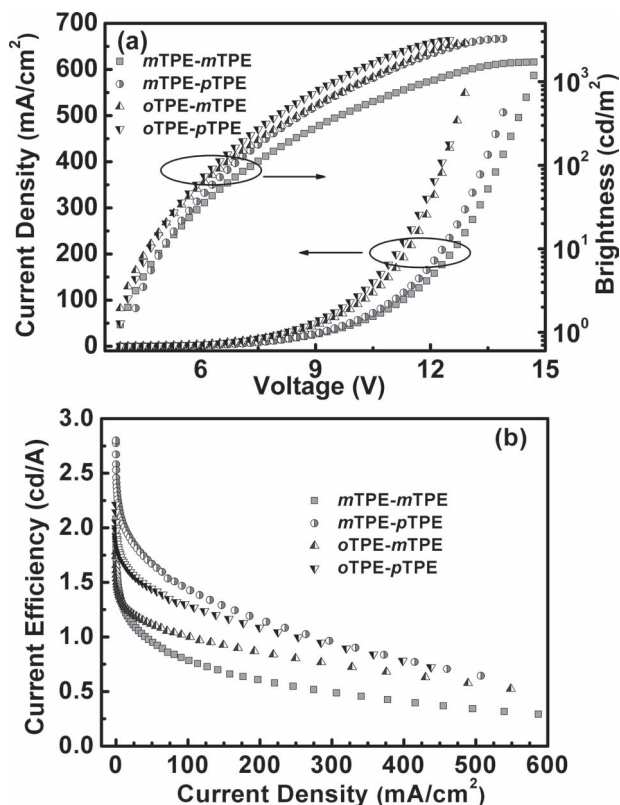


Figure 5. a) Current density–voltage–luminance characteristics of multilayer EL devices of *m*TPE-*p*TPE, *m*TPE-*m*TPE, *o*TPE-*m*TPE, and *o*TPE-*p*TPE. b) Change in current efficiency with the current density in multilayer EL devices. Device configurations: ITO/MoO₃ (10 nm)/NPB (60 nm)/EML (15 nm)/TPBi (35 nm)/LiF (1 nm)/Al.

Accompanying the increase of the voltage, the luminance increases rapidly. Among them, *m*TPE-*p*TPE exhibits the best EL performance, with a maximum luminance (L_{max}) of 3266 cd m⁻², a maximum current efficiency ($\eta_{\text{C, max}}$) of 2.8 cd A⁻¹ and a maximum power efficiency ($\eta_{\text{P, max}}$) of 2.0 lm W⁻¹, which are more than 1.5-fold higher than the values achieved by *o*TPE-*m*TPE. Good EL efficiencies were obtained from devices of *o*TPE-*p*TPE and *m*TPE-*m*TPE, with L_{max} , $\eta_{\text{C, max}}$, and $\eta_{\text{P, max}}$ of 3166 cd m⁻², 2.2 cd A⁻¹, and 1.8 lm W⁻¹; and, 1718 cd m⁻², 2.1 cd A⁻¹, and 1.7 lm W⁻¹, respectively. The EL emission of the original *p*TPE (BTPE) reported in the literature, was tuned from the sky-blue to deep-blue in our new BTPE derivatives, realizing the control of light emission through a very simple strategy with minor structural modification. In detail, all the four luminophors exhibit deep-blue emission (435–459 nm) when fabricated as emissive layers (Figure 6), compared to BTPE with sky-blue emission peaked at 488 nm. Especially, the EL spectrum of *o*TPE-*m*TPE is peaked at 435 nm with CIE chromaticity coordinates of (0.16, 0.14), which is even 10 nm blue-shifted compared to TPE (445 nm). This should be ascribed to its highly twisted geometric structure as mentioned above, in addition to the controlled conjugated effect derived from the different linkage positions. The highly twisted geometric structure makes *o*TPE-*m*TPE more easily crystallized when serving as emitter; that is, crystallization will cause blue-shifted emission. In addition, as *m*TPE-*p*TPE owns more planar conformation, its EL spectrum is more red-shifted, with EL peak at 459 nm and CIE chromaticity coordinates of (0.16, 0.16), than those of *o*TPE-*p*TPE and *m*TPE-*m*TPE, with values of 454 nm, (0.16, 0.14); and, 452 nm, (0.15, 0.11), respectively. The satisfactory EL efficiencies and deep-blue emission should be ascribed to the different conjugation degree of *ortho*-, *meta*-, or *para*- linkage, which could effectively tune the conjugated effects of two simple TPE units, though the device configuration is yet to be optimized. As *m*TPE-*p*TPE, which is more conjugated than the other three emitters, possesses the best EL efficiencies while still emitting in the deep-blue region, it further indicates that the balance between high efficiencies and effective conjugation length could be adjusted. On one hand, once the conjugation is almost disrupted, such as *o*TPE-*m*TPE, it may result in poor EL performance; on the other hand, if the conjugation is prolonged too much, like BTPE, the EL spectrum will be red-shifted to a large extent; our preliminary results confirmed that, by intelligently modifying the subtle structure of AIE luminophors, a balance can be partially achieved.

3. Conclusions

In summary, four BTPE derivatives, namely *o*TPE-*m*TPE, *o*TPE-*p*TPE, *m*TPE-*m*TPE, and *m*TPE-*p*TPE, were successfully obtained with the aim of generating deep-blue emitters in OLED devices. By utilizing the different conjugated effect of *ortho*-, *meta*-, and *para*- linkage of two TPE units, the prolonged π -conjugation length could be partially shortened, realizing the control of light emission through a very simple strategy with minor structural modification. When fabricated as emissive layers in OLEDs, all the four luminogens exhibit deep blue emissions from 435 to 459 nm with L_{max} and $\eta_{\text{C, max}}$ up to

Table 2. EL performances of *m*TPE-*p*TPE, *m*TPE-*m*TPE, *o*TPE-*m*TPE, and *o*TPE-*p*TPE.

	λ_{EL} [nm]	V_{on}^{a} [V]	$L_{\text{max}}^{\text{b}}$ [cd m ⁻²]	$\eta_{\text{P, max}}^{\text{c}}$ [lm W ⁻¹]	$\eta_{\text{C, max}}^{\text{c}}$ [cd A ⁻¹]	$\eta_{\text{ext, max}}^{\text{c}}$ [%]	CIE ^d (x, y)
<i>m</i> TPE- <i>m</i> TPE	452	3.9	1718	1.7	2.1	1.9	(0.15, 0.11)
<i>m</i> TPE- <i>p</i> TPE	459	4.1	3266	2.0	2.8	1.9	(0.16, 0.16)
<i>o</i> TPE- <i>m</i> TPE	435	3.7	2883	1.4	1.8	1.4	(0.16, 0.14)
<i>o</i> TPE- <i>p</i> TPE	454	3.9	3166	1.8	2.2	1.7	(0.16, 0.14)

^a V_{on} is the turn-on voltage at 1 cd m⁻²; ^b L_{max} the maximum luminance; ^c $\eta_{\text{C, max}}$, $\eta_{\text{C, max}}$, and $\eta_{\text{ext, max}}$ the maximum power, current, and external efficiencies, respectively; ^dCIE coordinates at 100 mA cm⁻².

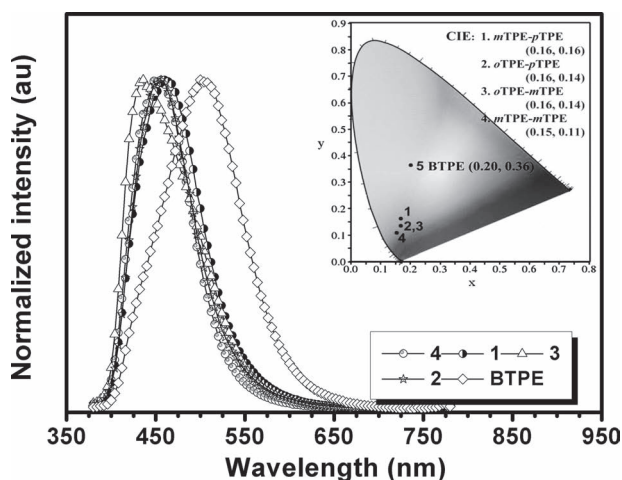


Figure 6. EL spectra of *m*TPE-*p*TPE (1), *m*TPE-*m*TPE (4), *o*TPE-*m*TPE (3), *o*TPE-*p*TPE (2), and BTPE. Inset: CIE chromaticity coordinates of the four luminogens.

3266 cd m⁻² and 2.8 cd A⁻¹, and CIE chromaticity coordinates of (0.16, 0.14), (0.15, 0.11), (0.16, 0.14), and (0.16, 0.16), respectively. In comparison with BTPE (*p*TPE-*p*TPE), the structures of our newly prepared BTPE derivatives, *o*TPE-*m*TPE, *o*TPE-*p*TPE, *m*TPE-*m*TPE, and *m*TPE-*p*TPE, are similar. But, their EL performance, especially the emission color, is different. Actually, a minor or even apparently negligible structural modification is an intelligent utilization of the basic conjugative effect; thus, the four luminophors reported here are totally different from the original *p*TPE-*p*TPE reported in the literature, although their structures are similar. It is hoped that this design idea may stimulate the flourishing development of AIE luminophors with controllable emission, and many previously reported TPE-based emitters should be re-investigated, just changing the linkage positions of the aromatic blocks as described here.

4. Experimental Section

Characterization: ¹H and ¹³C NMR spectra were measured on a MECUYRVX300 spectrometer. Mass spectra were measured on a ZAB 3F-HF mass spectrophotometer. Matrix-assisted laser desorption ionization time-of-flight mass spectra were measured on a Voyager-DESTR MALDI-TOF mass spectrometer (MALDI-TOF MS; ABI,

American) equipped with a 337 nm nitrogen laser and a 1.2 m linear flight path in positive ion mode, or a GCT premier CAB048 mass spectrometer. UV-vis absorption spectra were recorded on a Shimadzu UV-2500 recording spectrophotometer. Photoluminescence spectra were recorded on a Hitachi F-4500 fluorescence spectrophotometer. Differential scanning calorimetry (DSC) was performed on a Mettler Toledo DSC 822e at a heating and cooling rate of 15 °C min⁻¹ from room temperature to 180 °C under argon. The glass transition temperature (T_g) was determined from the second heating scan. Thermogravimetric analysis (TGA) was undertaken with a NETZSCH STA 449C instrument. The thermal stability of the samples under a nitrogen atmosphere was determined by measuring their weight loss while heating at a rate of 10 °C min⁻¹ from 25 to 600 °C. Cyclic voltammetry (CV) was carried out on a CHI voltammetric analyzer in a three-electrode cell with a Pt counter electrode, a Ag/AgCl reference electrode, and a glassy carbon working electrode at a scan rate of 100 mV s⁻¹ with 0.1 M tetrabutylammonium perchlorate (purchased from Alfa Aesar) as the supporting electrolyte, in anhydrous dichloromethane solution purged with nitrogen. The potential values obtained in reference to the Ag/Ag⁺ electrode were converted to values versus the saturated calomel electrode (SCE) by means of an internal ferrocenium/ferrocene (Fc⁺/Fc) standard.

Computational Details: The geometrical and electronic properties were optimized at B3LYP/6-31g(d) level using Gaussian 09 program. The molecular orbitals were obtained at the same level of theory.

OLED Device Fabrication and Measurement: The hole-transporting material NPB (1,4-bis(1-naphthylphenylamino)-biphenyl) and electron-transporting material 1,3,5-tris(*N*-phenylbenzimidazol-2-yl)benzene (TPBI) were obtained from a commercial source. The EL devices were fabricated by vacuum deposition of the materials at a base pressure of 10⁻⁶ Torr onto glass precoated with a layer of indium tin oxide (ITO) with a sheet resistance of 25 Ω per square. Before deposition of an organic layer, the clear ITO substrates were treated with oxygen plasma for 2 min. The deposition rate of organic compounds was 1–2 Å s⁻¹. Finally, a cathode composed of lithium fluoride (1 nm) and aluminum (100 nm) was sequentially deposited onto the substrate in the vacuum of 10⁻⁶ Torr. The *L*-*V*-*J* of the devices was measured with a Keithley 2400 Source meter and a Keithley 2000 Source multimeter equipped with a calibrated silicon photodiode. The EL spectra were measured by JY SPEX CCD3000 spectrometer. All measurements were carried out at room temperature under ambient conditions.

Preparation of Compounds: All other chemicals and reagents were obtained from commercial sources and used as received without further purification. Solvents for chemical synthesis were purified according to the standard procedures. Compound 1, *p*TPE-Br and Compound 4 were synthesized according to the literature.^[12]

Synthesis of Compound 2: 2-Aminobenzophenone (3.92 g, 20.0 mmol) was dissolved in HBr (20 mL, 47% in H₂O), cooled to 0 °C, and an aqueous solution (5 mL) of NaNO₂ (1.52 g, 22 mmol) was added dropwise. After 30 min, the reaction mixture was allowed to warm to room temperature, stirred for another hour. This suspension was then added with vigorous stirring to CuBr (3.59 g, 25 mmol) dissolved in 15 mL of HBr. The reaction mixture was heated to 60 °C for 1 h, afterwards

poored on iced water (100 mL) and extracted with dichloromethane. The combined organic fractions were washed with brine (100 mL), dried over MgSO_4 , filtered and concentrated in vacuo. The crude product was purified by chromatography using petroleum ether/dichloromethane (3:1 v/v) as eluent to obtain a yellow oil in the yield of 65% (3.4 g). ^1H NMR (300 MHz, CDCl_3) δ (ppm): 7.83–7.1 (m, 2H), 7.66–7.61 (m, 2H), 7.47–7.36 (m, 5H).

Synthesis of mTPE-Br: A 2.3 M solution of *n*-butyllithium in hexane (4.09 mmol, 1.78 mL) was added to a solution of diphenylmethane (0.86 g, 5.12 mmol) in anhydrous tetrahydrofuran (40 mL) at 0 °C under an atmosphere of argon. After stirring for 1 h at this temperature, 3-bromobenzophenone (0.89 g, 3.41 mmol) was added. After 2 h, the mixture was slowly warmed to room temperature. Then, the reaction was quenched with an aqueous solution of ammonium chloride and the mixture was extracted with dichloromethane. The organic layer was evaporated after drying with anhydrous sodium sulfate, and the resulting crude product was dissolved in toluene (25 mL). The *p*-toluenesulfonic acid (0.12 g, 0.68 mmol) was added, and the mixture was refluxed overnight and cooled to room temperature. The mixture was evaporated and the crude product was purified by silica gel column chromatography using petroleum ether as eluent to obtain a white powder in the yield of 50% (0.7 g). ^1H NMR (300 MHz, CDCl_3) δ (ppm): 7.20–7.11 (m, 11H), 7.02–7.01 (m, 5H), 6.96–6.95 (m, 2H). ^{13}C NMR (75 MHz, CDCl_3) δ (ppm): 146.0, 143.4, 143.3, 143.1, 142.2, 139.5, 134.2, 131.3, 130.1, 129.6, 129.3, 128.0, 127.8, 126.9, 126.8, 121.9. MS (EI), m/z : 412.13 ($[\text{M}^+]$, calcd. for $\text{C}_{26}\text{H}_{19}\text{Br}$: 411.33).

Synthesis of oTPE-Br: Prepared according to a similar procedure for mTPE-Br from Compound 2. White powder. Yield: 30%. ^1H NMR (300 MHz, CDCl_3) δ (ppm): 7.17–7.03 (m, 19H). MS (EI), m/z : 412.10 ($[\text{M}^+]$, calcd. for $\text{C}_{26}\text{H}_{19}\text{Br}$: 411.33).

Synthesis of Compound 3: A 2.3 M solution of *n*-butyllithium in hexane (15.0 mmol, 6.5 mL) was added to a solution of mTPE-Br (4.12 g, 10.0 mmol) in anhydrous tetrahydrofuran (60 mL) at –78 °C under an atmosphere of argon. After stirring for 4 h, 2-isopropoxy-4,4,5,5-tetramethyl-1,3,2-dioxaborolane (6.1 mL) was added. After 2 h, the mixture was slowly warmed to room temperature. After stirring overnight, the reaction was terminated by the added brine. The mixture was extracted with dichloromethane, and the combined organic layer was dried over anhydrous sodium sulfate. After filtration and solvent evaporation, the crude product was purified by silica gel column chromatography using petroleum ether/dichloromethane (5:1 v/v) as eluent. White powder of 3 was obtained in the yield of 60% (2.30 g). ^1H NMR (300 MHz, CDCl_3) δ (ppm): 7.53–7.48 (m, 2H), 7.09–7.02 (m, 17H), 1.28 (s, 12H). ^{13}C NMR (75 MHz, CDCl_3) δ (ppm): 143.6, 143.3, 142.9, 141.1, 140.8, 137.5, 134.2, 132.7, 131.3, 131.2, 127.5, 127.0, 126.3, 126.2, 83.6, 24.7. MS (EI), m/z : 458.35 ($[\text{M}^+]$, calcd for $\text{C}_{32}\text{H}_{31}\text{BO}_2$, 458.40).

General Procedure for the Synthesis of Compounds mTPE-pTPE, mTPE-mTPE, oTPE-mTPE and oTPE-pTPE: mTPE-mTPE: A mixture of mTPE-Br (412 mg, 1 mmol), compound 3 (459 mg, 1 mmol), $\text{Pd}(\text{PPh}_3)_4$ (0.10 g, 4% mmol), and potassium hydroxide (236 mg, 5 mmol) in 15 mL of THF and 3 mL of distilled water in a 50 mL Schlenk tube was refluxed for 2 d under argon. The mixture was extracted with dichloromethane. The combined organic extracts were dried over anhydrous Na_2SO_4 and concentrated by rotary evaporation. The crude product was purified by column chromatography on silica gel using dichloromethane/petroleum ether (1:5 v/v) as eluent to afford the product as a white powder in the yield of 61.2% (320 mg). ^1H NMR (300 MHz, CDCl_3) δ (ppm): 7.09–7.04 (m, 32H), 6.97–6.92 (m, 6H). ^{13}C NMR (75 MHz, CDCl_3) δ (ppm): 144.0, 143.9, 143.7, 141.5, 141.2, 140.5, 131.6, 130.6, 130.2, 128.1, 127.9, 126.7, 125.4. MS (EI), m/z : 662.70 ($[\text{M}^+]$, calcd. for $\text{C}_{52}\text{H}_{38}$: 662.86). HRMS: m/z for $\text{C}_{52}\text{H}_{38}$ [$\text{M}+\text{NH}_4^+$], calcd.: 680.3312; found: 680.3307.

mTPE-pTPE: White powder. Yield: 65%. ^1H NMR (300 MHz, CDCl_3) δ (ppm): 7.09–6.98 (m, 38H). ^{13}C NMR (75 MHz, CDCl_3) δ (ppm): 144.2, 144.1, 143.9, 143.8, 142.8, 141.5, 141.3, 141.1, 140.8, 140.1, 139.1, 131.8, 131.6, 130.5, 130.4, 128.3, 128.0, 127.9, 126.7, 126.4, 125.3. MS (EI), m/z : 662.79 ($[\text{M}^+]$, calcd. for $\text{C}_{52}\text{H}_{38}$: 662.86). HRMS: m/z for $\text{C}_{52}\text{H}_{38}$ [$\text{M}+\text{NH}_4^+$], calcd.: 680.3312; found: 680.3322.

oTPE-pTPE: White powder. Yield: 48%. ^1H NMR (300 MHz, CDCl_3) δ (ppm): 7.13–6.80 (m, 36H), 6.46–6.43 (m, 2H). ^{13}C NMR (75 MHz, CDCl_3) δ (ppm): 144.2, 143.4, 142.2, 141.1, 139.9, 138.9, 133.0, 131.6, 130.9, 130.7, 128.5, 128.0, 127.6, 127.2, 127.0, 126.7. MS (EI), m/z : 662.40 ($[\text{M}^+]$, calcd. for $\text{C}_{52}\text{H}_{38}$: 662.86). HRMS: m/z for $\text{C}_{52}\text{H}_{38}$ [$\text{M}+\text{NH}_4^+$], calcd.: 680.3312; found: 680.3334.

oTPE-mTPE: White powder. Yield: 40%. ^1H NMR (300 MHz, CDCl_3) δ (ppm): 7.08–6.88 (m, 33H), 6.81–6.78 (m, 2H), 6.64–6.61 (m, 3H). ^{13}C NMR (75 MHz, CDCl_3) δ (ppm): 144.0, 141.2, 139.8, 137.5, 132.2, 131.6, 131.3, 130.3, 130.0, 129.1, 128.1, 127.9, 126.9, 126.7, 122.7. MS (EI), m/z : 662.42 ($[\text{M}^+]$, calcd. for $\text{C}_{52}\text{H}_{38}$: 662.86). HRMS: m/z for $\text{C}_{52}\text{H}_{38}$ [$\text{M}+\text{NH}_4^+$], calcd.: 680.3312; found: 680.3319.

Crystallographic data (excluding structure factors) for the structure(s) reported in this paper have been deposited with the Cambridge Crystallographic Data Centre as supplementary publication nos. CCDC-894519 and 894520.

Supporting Information

Supporting Information is available from the Wiley Online Library or from the author.

Acknowledgements

Z.L. is grateful to the National Science Foundation of China (no. 21161160556), the National Fundamental Key Research Program (2011CB932702, 2013CB834700), and the Open Project of State Key Laboratory of Supramolecular Structure and Materials (sklssm201219) for financial support. D.M. is grateful to the Science Fund for Creative Research Groups of NSFC (20921061), and the National Natural Science Foundation of China (50973104, 60906020) for financial support.

Received: September 12, 2012

Published online: December 4, 2012

- a) C. W. Tang, S. A. Vanslyke, *Appl. Phys. Lett.* **1987**, *51*, 913; b) C. Adachi, T. Tsutsui, S. Saito, *Appl. Phys. Lett.* **1989**, *55*, 1489; c) M. A. Baldo, M. E. Thompson, S. R. Forrest, *Nature* **2000**, *403*, 750; d) B. W. D'Andrade, S. R. Forrest, *Adv. Mater.* **2004**, *16*, 1585.
- a) K. C. Wu, P. J. Ku, C. S. Lin, H. T. Shih, F. I. Wu, M. J. Huang, J. J. Lin, I. C. Chen, C. H. Cheng, *Adv. Funct. Mater.* **2008**, *18*, 67; b) I. Cho, S. H. Kim, J. H. Kim, S. Park, S. Y. Park, *J. Mater. Chem.* **2012**, *22*, 123; c) S. H. Kim, I. Cho, M. K. Sim, S. Park, S. Y. Park, *J. Mater. Chem.* **2011**, *21*, 9139; d) H. Park, J. Lee, I. Kang, H. Y. Chu, J. I. Lee, S. K. Kwon, Y. H. Kim, *J. Mater. Chem.* **2012**, *22*, 2695.
- a) L. M. Leung, W. Y. Lo, S. K. So, K. M. Lee, W. K. Choi, *J. Am. Chem. Soc.* **2000**, *122*, 5640; b) R. J. Tseng, R. C. Chiechi, F. Wudl, Y. Yang, *Appl. Phys. Lett.* **2006**, *88*, 093512; c) T. P. I. Saragi, T. Spehr, A. Siebert, T. Fuhrmann-Lieker, J. Salbeck, *Chem. Rev.* **2007**, *107*, 1011; d) Y. Y. Lyu, J. Kwak, O. Kwon, S. H. Lee, D. Kim, C. Lee, K. Char, *Adv. Mater.* **2008**, *20*, 2720; e) K. T. Kamtekar, A. P. Monkman, M. R. Bryce, *Adv. Mater.* **2010**, *22*, 572.
- a) Y.-H. Kim, H.-C. Jeong, S.-H. Kim, K. Yang, S.-K. Kwon, *Adv. Funct. Mater.* **2005**, *15*, 1799; b) S.-K. Kim, Y.-I. Park, I.-N. Kang, J.-W. Park, *J. Mater. Chem.* **2007**, *17*, 4670; c) S.-K. Kim, B. Yang, Y. Ma, J.-H. Lee, J.-W. Park, *J. Mater. Chem.* **2008**, *18*, 3376.
- a) C.-C. Wu, Y.-T. Lin, K.-T. Wong, R.-T. Chen, Y.-Y. Chien, *Adv. Mater.* **2004**, *16*, 61; b) T.-C. Chao, Y.-T. Lin, C.-Y. Yang, T. S. Hung, H.-C. Chou, C.-C. Wu, K.-T. Wong, *Adv. Mater.* **2005**, *17*, 992; c) T. Zhang, D. Liu, Q. Wang, R. Wang, H. Ren, J. Li, *J. Mater. Chem.* **2011**, *21*, 12969.

- [6] a) M.-T. Lee, C.-H. Liao, C.-H. Tsai, C. H. Chen, *Adv. Mater.* **2005**, *17*, 2493; b) Y. Duan, Y. Zhao, P. Chen, J. Li, S. Liu, F. He, Y. Ma, *Appl. Phys. Lett.* **2006**, *88*, 263503.
- [7] P.-I. Shih, C.-Y. Chuang, C.-H. Chien, E. W.-G. Diau, C.-F. Shu, *Adv. Funct. Mater.* **2007**, *17*, 3141.
- [8] a) S. W. Thomas III, G. D. Joly, T. M. Swager, *Chem. Rev.* **2007**, *107*, 1339; b) A. C. Grimsdale, K. L. Chan, R. E. Martin, P. G. Jokisz, A. B. Holmes, *Chem. Rev.* **2009**, *109*, 897.
- [9] a) J. Luo, Xie, J. W. Y. Lam, L. Cheng, H. Chen, C. Qiu, H. S. Kwok, X. Zhan, Y. Liu, D. Zhu, B. Z. Tang, *Chem. Commun.* **2001**, 1740; b) Y. Hong, J. W. Y. Lam, B. Z. Tang, *Chem. Commun.* **2009**, 4332.
- [10] a) B. K. An, J. Gierschner, S. Y. Park, *Acc. Chem. Res.* **2012**, *45*, 544; b) M. Wang, G. Zhang, D. Zhang, D. Zhu, B. Z. Tang, *J. Mater. Chem.* **2010**, *20*, 1858.
- [11] a) Y. Dong, J. W. Y. Lam, A. Qin, J. Liu, Z. Li, B. Z. Tang, J. Sun, H. S. Kwok, *Appl. Phys. Lett.* **2007**, *91*, 011111; b) S. K. Kim, Y. Park, I. N. Kang, J. W. Park, *J. Mater. Chem.* **2007**, *17*, 4670; c) W. Z. Yuan, P. Lu, S. Chen, J. W. Y. Lam, Z. Wang, Y. Liu, H. S. Kwok, Y. Ma, B. Z. Tang, *Adv. Mater.* **2010**, *22*, 2159; d) Z. Zhao, Jacky W. Y. Lam, C. Y. K. Chan, S. Chen, J. Liu, P. Lu, M. Rodriguez, J. L. Maldonado, G. Ramos-Ortiz, H. H. Y. Sung, I. D. Williams, H. Su, K. S. Wong, Y. Ma, H. S. Kwok, H. Qiu, B. Z. Tang, *Adv. Mater.* **2011**, *23*, 5430; e) C. Y. K. Chan, Z. Zhao, J. W. Y. Lam, J. Liu, S. Chen, P. Lu, F. Mahtab, X. Chen, H. H. Y. Sung, H. S. Kwok, Y. Ma, I. D. Williams, K. S. Wong, B. Z. Tang, *Adv. Funct. Mater.* **2012**, *22*, 378.
- [12] Z. Zhao, S. Chen, X. Shen, F. Mahtab, Y. Yu, P. Lu, J. W. Y. Lam, H. S. Kwok, B. Z. Tang, *Chem. Commun.* **2010**, 46, 686.
- [13] a) J. Huang, X. Yang, J. Wang, C. Zhong, L. Wang, J. Qin, Z. Li, *J. Mater. Chem.* **2012**, *22*, 2478; b) J. Huang, N. Sun, J. Yang, R. Tang, Q. Li, D. Ma, J. Qin, Z. Li, *J. Mater. Chem.* **2012**, *22*, 12001.
- [14] P. I. Shih, C. Y. Chuang, C. H. Chien, E. W. G. Diau, C. F. Shu, *Adv. Funct. Mater.* **2007**, *17*, 3141.
- [15] a) Y. Dong, J. W. Y. Lam, Z. Li, A. Qin, H. Tong, Y. Dong, X. Feng, B. Z. Tang, *J. Inorg. Organomet. Polym. Mater.* **2005**, *15*, 287; b) H. Tong, Y. Hong, Y. Dong, Y. Ren, M. Haeussler, J. W. Y. Lam, K. S. Wong, B. Z. Tang, *J. Phys. Chem. B* **2007**, *111*, 2000; c) H. Tong, Y. Dong, Y. Hong, M. Haeussler, J. W. Y. Lam, H. H. Y. Sung, X. Yu, J. Sun, I. D. Williams, H. S. Kwok, B. Z. Tang, *J. Phys. Chem. C* **2007**, *111*, 2287; d) H. Tong, Y. Hong, Y. Dong, M. Haeussler, Z. Li, J. W. Y. Lam, Y. Dong, H. H. Y. Sung, I. D. Williams, B. Z. Tang, *J. Phys. Chem. B* **2007**, *111*, 11817.